Comparative calorimetric studies on the dynamic conformation of plant 5S rRNA: II structural interpretation of the thermal unfolding patterns for lupin seeds and wheat germ

T.Kuliński, M.D.Bratek-Wiewiórowska, M.Wiewiórowski, A.Zielenkiewicz[1], M.Żółkiewski[1] and W.Zielenkiewicz[1]

Institute of Bioorganic Chemistry, Polish Academy of Sciences, Noskowskiego 12/14, 61-704 Poznań and [1]Institute of Physical Chemistry, Polish Academy of Sciences, Kasprzaka 44/52, 01-224 Warsaw, Poland

ABSTRACT

Thermal unfolding of 5S rRNA from wheat germ (WG) and lupin seeds (LS) was studied in solution. Experimental curves of differential scanning calorimetry (DSC) were resolved into particular components according to the thermodynamic model of two-state transitions. The DSC temperature profiles for WG and LS differ significantly in spite of very high similarities in the sequence of both molecules. Those results are interpreted according to a model of the secondary and tertiary molecular structure of 5S rRNA. A comparison of the 'nearest neighbour' model of interaction with the experimental thermodynamic results enables a complete interpretation of the process of the melting of its structures. In light of our observations, the crucial differences between both DSC melting profiles are mainly an outcome of different thermodynamic properties of the first helical fragment 'A' made up of 9 complementary base pairs. It contains 6 differences in the nucleotide sequence of both types of molecules, which still retain 9-meric double helixes. The temperature stability of his helix in WG is much lower than of the LS one. Moreover, the results supply evidence for a strong specific tertiary interaction between the two hairpin loops 'c' and 'e' in both 5S rRNA molecules, modulated by small differences in the thermodynamic properties of both 5S rRNA.

INTRODUCTION

5S rRNA is an essential component of the ribosome in prokaryotic and eukaryotic organisms [1], so its secondary and tertiary structures have been the objects of intensive studies. The numerous nucleotide sequences collected so far, have led to the construction of a general model of the secondary structure, based mostly on a comparative analysis of the already determined sequences [2], but the problem of its conformational dynamics still remains open. Tertiary interactions, which organize the

spatial structure of the molecule have also been postulated [3,4]. Information about the structure of 5S rRNA in solution is obtained by biochemical methods such as enzymatic digestion, oligonucleotide bindings, etc. But even with the help of advanced NMR spectroscopy and crystallographic studies, it has not been possible to solve the problem of 5S rRNA spatial structure. The quality of 5S rRNA crystals obtained so far is not satisfactory enough to supply information on the molecular structure of 5S rRNA [5].

Numerous observations show that 5S rRNA adopts various conformations in solution, depending on the concentration and type of counter ions, temperature and urea concentration. 5S rRNA from E.coli can occur in two forms: A—native, and B—denatured by temperature or by urea [6]. The transformation into either form is reversible. Some hypotheses claim that both forms of 5S rRNA have a functional significance for the process of protein biosynthesis [7]. Optical spectroscopic studies and NMR data indicate that the presence of Mg^{2+} brings about a tertiary conformational change in the native form A [8]. Out of the many physical techniques used for studying the dynamics of 5S rRNA structure, differential scanning calorimetry (DSC) is especially valuable, since it supplies direct data on the thermodynamic stability of the molecule in solution.

The DSC measurements have already been performed for 5S rRNA from E.coli, B.subtilis, wheat germ [9,10,11] and by us for 5S rRNA from WG and LS [12]. Both those plant 5S rRNA show minor differences in the primary nucleotide sequences [13,14], and the sites of the differences seem to indicate an identity, or high similarity of the secondary and tertiary structures. However, their melting profiles are significantly different [12]. On the basis of the latter, it was possible to draw some introductory assumptions about factors which stabilize the structures of both molecules.

The aim of this paper is to substantially extend the interpretation of the experimental results and to give a precise analysis of the DSC curves, so as to correlate them with the thermodynamic properties deduced from the predicted secondary structure and

Table 1. Thermodynamic parameters of particular component two-state transitions (cmpt) numerically derived from experimental DSC profiles for 5S rRNA from wheat germ WG and lupin seeds LS in the basic buffer.

No. of cmpt	WG				LS			
	T_m [K]	($°C$)	ΔH [kcal/mol]	ΔG	T_m [K]	($°C$)	ΔH [kcal/mol]	ΔG
1	325	(52)	87.6	−4.04	328.8	(55.8)	70.2	−4.18
2	320	(47)	112.8	−7.44	323.5	(50.5)	147.4	−6.10
3	315	(42)	95.9	−1.52	320.0	(47.0)	52.7	−2.25
4	308	(35)	70.0	0.68	308.5	(35.5)	101.0	0.50
5					301.0	(28.0)	27.1	0.20
Total			366.3	−12.3			398.1	−11.8

T_m—melting temperature of the two-state transition
ΔH—enthalpy of this transition
ΔG—free energy for the component transition calculated for the temperature $T = 310$ K.
Total—sum of ΔH or ΔG

potential tertiary interactions, confirming in this way the postulated structural models, or introducing to them the necessary modifications.

MATERIALS AND METHODS

5S rRNAs were isolated from Lupinus luteus [LS] and wheat germ [WG] as previously described by multiple gel filtration on Sephadex G75 [13,14] and then further purified on DEAE-cellulose. The purity of the products was verified by gel electrophoresis. 5S rRNA lyophilized preparations were dissolved in a selected buffer and dialyzed against the same buffer. Buffer of pH = 7.2 contained 10 mM sodium cacodylate, 1 mM Na_2EDTA and 20 mM NaCl. The concentration of samples used for measurements was 3.0×10^{-8} mole/ml. The extinction coefficient used was 10.29×10^5 M^{-1} for LS and 10.03×10^5 M^{-1} for WG.

Measurements of specific heat in the temperature function were taken on a DASM-1M differential scanning calorimeter (USSR) [15]. The temperature range studied was $287-380$ K with scanning speed 1 K/min.

Since the specific heat values for the native and completely denatured forms of 5S rRNA are significantly dissimilar, it was necessary to make assumptions about the forms of the dependence of the calorimetric base line on temperature in the region of conformational change. Because of a stepwise character of the change, it was assumed that the base line could be approximated by a straight line connecting those points before and after the change at which the diagram became markedly non-linear.

Upon determination of the base line, the obtained curves were analyzed with the help of iterative algorithm defined by Freire and Biltonen [16]. The results were then used as starting parameters for a numerical fitting of the function reflecting Cp(T,) which was a sum of independent two-state transitions, to experimental data [17].

The analysis of the secondary structure was done with the PC-FOLD computer program [18,19], on an IBM PC AT computer. The thermodynamic parameters used in structural calculations were in accordance with Turner [3,20].

RESULTS

Differential scanning calorimetry

Experimental results of DSC measurements are shown in Table 1 and in Figs. 1a−1b. The figures present the experimentally
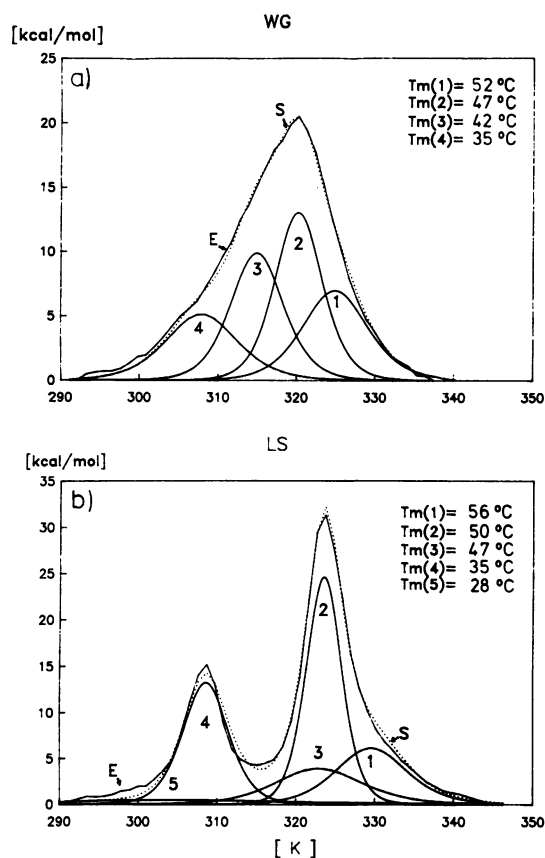
Fig. 1. DSC plot of 5S rRNA from wheat germ (WG)—a, and from lupin seeds (LS)—b in the standard buffer. Curve E presents experimental heat capacity in the function of the temperature (in [K]) after base line subtraction. Curves 1−4 represents particular component thermodynamic transitions simulated by numerical analysis of the experimental data, and curve S presents their sum. Transition temperatures (T_m) show the position of the maximum of the component transitions.

determined dependence of the specific heat value on the temperature. The region below the DSC curve is the total enthalpy ΔH of the melting of the structure. In the case of complex structural transformations, as it is in the case of 5S rRNA the DSC curve has to be decomposed into particular phase transitions characterized by appropriate contributions of enthalpy ΔH and transition temperatures T_m. The figure for each experiment

Table 2. The values of enthalpy (ΔH) and relative temperature stability (T_m) evaluated theoretically for double helical fragments of 5S rRNA from lupin seeds LS and wheat germ WG according to the 2D and 3D structure presented in Fig.2a/2b for LS and in Fig.2c for WG.

	WG		LS	
helix	ΔH [kcal/mol]	T_m [K] (°C)	ΔH [kcal/mol]	T_m [K] (°C)
A	56.6	320 (47)	66.5	331 (58)
B	75.0	324 (51)	75.0	324 (51)
C	43.2	318 (45)	27.8	317 (44)
C_L	–	–	38.5	316 (43)
D	46.5	313 (40)	46.5	313 (40)
E	61.1	322 (49)	61.1	322 (49)
C'	28.4	300 (27)	21.0	308 (35)
C'_L	–	–	59.0	298 (25)
D'	11.0	–	11.0	–
T1	34.9	317 (44)	34.9	317 (44)
T2	3.0	–	3.0	–
Total ΔH	355.0		385.0	

ΔH denotes the values of the enthalpy calculated theoretically, including the stabilising contribution of the unpaired nucleotides at the ends of helical fragments ('dangling ends').

T_m are theoretically estimated only for the model including the 'dangling ends' contribution to the stability of structure D.
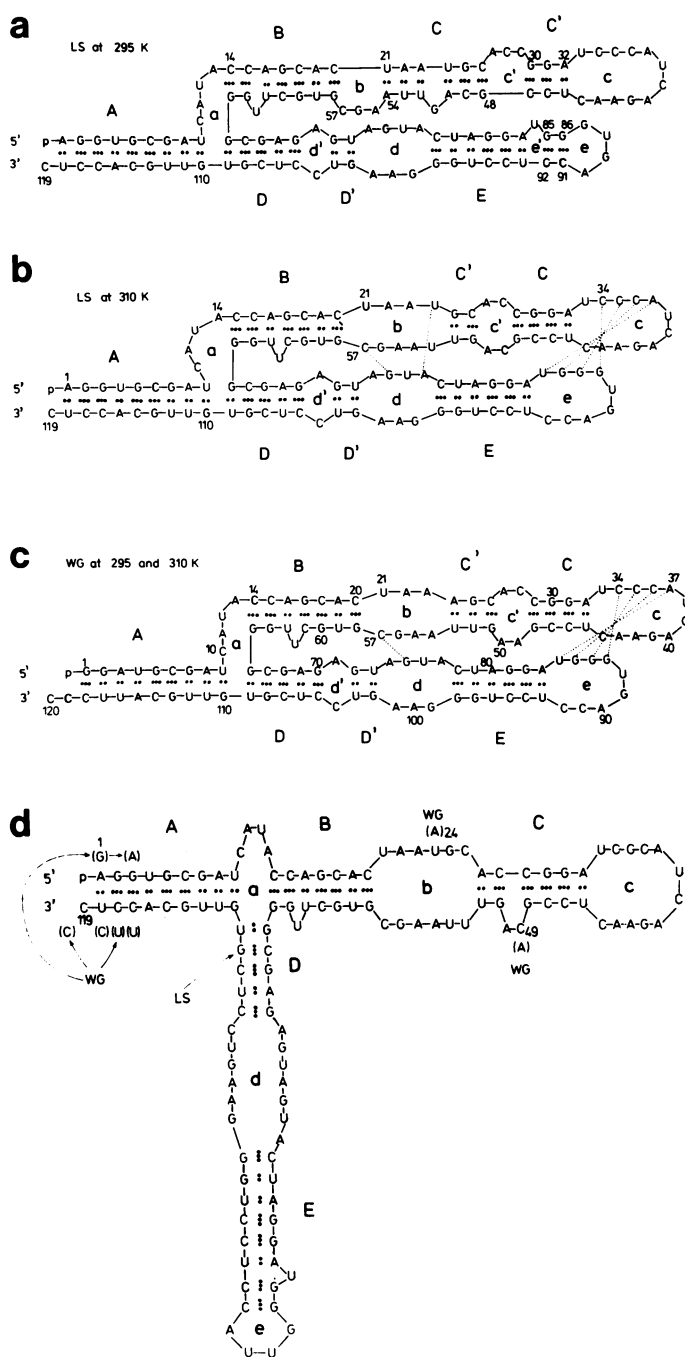
C_L and C'_L helices present in the structure in low temperature 5S rRNA of LS are shown in Fig 2a.

a LS at 295 K

b LS at 310 K

c WG at 295 and 310 K

d

Fig. 2. Postulated secondary structure of 5S rRNA: a) from lupin seeds in low temperature (295 K), b) from lupin seeds in high temperature (310 K), c) from wheat germs (the same in 295 and 310 K) Double helical regions are marked with capitals (A−E), loops are assigned with small letters (a−e), postulated tertiary pairing with dotted lines; d) postulated secondary structure of 5S rRNA proposed by us previously [12], with marked differences in sequence between LS and WG.

comprises also the results of the decomposition of the experimental curve into component two-phase transitions. Their sum is depicted as a simulated curve which overlaps the experimental one, and it is therefore possible to evaluate to what extent the two curves are congruent.

For a series of 5S rRNA samples measured under identical conditions, the maximum difference between the values of a total enthalpy for complete phase transition did not exceeded 10%. However, curve analysis showed that the values of melting temperatures characteristic for particular two-state transitions and the proportions between the values of enthalpy corresponding to them were identical for all the samples within a series. The number of components present in the experimental curves was determined directly by a program analyzing the whole curves with the algorithm of Freire and Biltonen [16], although it cannot be excluded that components of two close T_m were not separated into independent transitions.

The melting profiles of 5S rRNA for WG and LS in basic buffer differed essentially. The melting of WG 5S rRNA proceeded evenly (see Fig. 1a), without any visible shoulders on the unique peak of DSC curve, whereas LS was characterized by two distinct peaks (see Fig. 1b). The DSC curve for WG 5S rRNA (Fig. 1a) after deconvolution shows four particular component transitions, each with an essential impact to ΔH enthalpy. Their summaric value was 366 kcal/mole versus 370 kcal/mole for total experimental enthalpy. The distribution of the temperatures of transition T_m was at a uniform rate, ranging from 308°K to 325°K (see Table 1 and Fig. 1a).

The decomposition of the DSC curve for LS 5S rRNA in basic buffer yielded five components (Fig. 1b and Table 1). The one with the lowest T_m equalling 301° had a relatively low value of enthalpy ΔH = 27.1 kcal/mole and was characterized by considerable half-width. The remaining components were well formed, and the simulated enthalpy value was 398.1 kcal/mole, versus experimental ΔH = 389.6 kcal/mole (see Table 1).

Modelling of the structure

In order to interpret the thermodynamic transitions observed by DSC, the possible secondary and tertiary structures of both 5S rRNA were carefully studied. The nucleotide sequences of 5S rRNA from LS and WG were already known [13,14]. They varied slightly, the differences being mostly located in one domain (see Table in ref [12] and Fig. 2d). To analyze the possible structural differences in the secondary and tertiary structures,

Table 3. Correlation of the experimental component two-state transitions (1−4) found in the DSC profiles with the theoretical melting of the model secondary and tertiary structural domain (A−T) of the 5S rRNA from WG.

DSC curve component	ΔH^{exp} [kcal/mol]	T_m^{exp} [K](°C)	Helical domain	ΔH^{teor} [kcal/mol]	T_m^{teor} [K](°C)
1	87.6	325 (52)	B	75.0	324 (51)
2	112.8	320 (47)	E	61.1	322 (49)
			C	43.2	318 (45)
3	95.9	315 (42)	A	56.1	320 (47)
			D	46.5	313 (40)
4	70.0	308 (35)	T1	34.9	317 (44)
			C'	28.4	298 (25)
			D'	11.0	280 (7)
			T2	3.0	—
Σ	366.3			359.2	

Table 4. Correlation of the experimental component two-states transitions (1−5) found in the DSC profiles with the theoretical melting of the model secondary and tertiary structural elements of 5S rRNA from lupin seeds (LS).

DSC curve component	ΔH^{exp} [kcal/mol]	T_m^{exp} [K](°C)	Helical domain	ΔH_m^{teor} [kcal/mol]	T_m^{teor} [K](°C)
1	70.2	329 (56)	A	66.5	331 (58)
2	147.4	323 (50)	B	75.0	324 (51)
			E	61.1	322 (49)
3	52.7	320 (47)	D	46.5	313 (40)
4	101.0	308 (35)	C	38.6	317 (44)
			T1	34.9	314 (41)
			C'	21.0	308 (35)
			D'	11.0	271 (−3)
5	27.1	301 (28)	$C_L'-C'$	27.0	298 (25)
			C_L-C		
Σ	388.1			381.8	

the former were first studied with a computer program predicting the RNA molecular structure [18] on the basis of a given sequence and empirical thermodynamic parameters for the possible intra-molecular interactions. Our analysis also took into consideration the altered thermodynamic parameters corresponding to a slightly stronger interaction between the terminal G-U pairs than between those located within the helix [20]. This interaction turned out to be crucial for selecting structures with minimal free energy. Having such parameters, the predicted secondary structures were isostructural for both 5S rRNA (with a minor difference in one pairing). If the terminal G-U pairing was omitted, very different secondary structures with minimal free energies were obtained.

The calculation of the minimum free energy of possible structures is usually performed with the parameters corresponding to a temperature of 310 K (37°C), which is taken as the standard for thermodynamic calculations for model oligonucleotides [3]. The melting temperatures for short helical fragments may often be lower than the standard temperature. This leads to a disappearance of structural features in the model structures considered. On the other hand, short helices interconnected with the whole molecular structure could still be still stable in temperatures higher than those predicted for separated helices. The starting temperature for calorimetric measurements was 15°C, but this experimental technique records only structural transitions characterized by a 'melting' temperature higher than the starting one. Therefore we analyzed the possible secondary structures with the free energy parameters transformed for the lower temperature, which was 22°C. In effect the structures found at this temperature differ slightly from the one predicted at 37°C , and contain some new paired fragments which are transformed into a single strand at 37°C.

The secondary structures presented in Figs. 2a−c, follow in an overall form the model generally accepted for 5S rRNA [2], but in structural details vary from the one previously proposed by us (Fig. 2d) [12].

The predicted structures (shown in Figs. 2a−2c) comprise 5 helices, each more than 3 nucleotides long, and 2 paired 2 or 3 nucleotide helical fragments. Within helical fragment 'A' there are 6 differences in the nucleotide sequence of the primary structures of both 5S rRNAs (compare Fig. 2a/2b with 2c and see Fig. 2d). The secondary structures of both sequences differ in the region which is stable only in low temperature (Figs. 2a and 2c).

The energetically preferred structure for LS 5S rRNA at 295 K (Fig. 2a) consists of a long six paired helix C_L' containing

strands U21-C26 with G48-A54, and a short three paired helix C_L (G30-A32 : U45-C47). At 310 K another 'high temperature' structure dominates energetically, with helix C identical as in WG, and helix C' consisting of two pairs only (Fig. 2b). Fragment C' comprises two nucleotides pairs in LS 5S rRNA (25−26)-(51−52) an three nucleotide pairs in WG due to a substitution of U(24) by A (see Fig. 2d). The remaining helical fragments are identical for both 5S rRNAs (compare Figs. 2b and 2c). At low temperature, pairing within hairpin loop 'e' namely G85-G86 : C91-C90 is also possible (see Fig. 2a).

Both types of 5S rRNA can potentially form a relatively strong tertiary interaction between hairpin-loop C and hairpin D of the sequence (34-CCCA-37): (84-UGGG-87) with a considerable enthalpy $\Delta H = -34.9$ kcal/mole. This tertiary interaction is competitive to the possible pairing (85−86):(91−92) inside hairpin loop e, but dominates almost three times ($\Delta G = -8.6$ kcal/mole) over it ($\Delta G = -2.9$ kcal/mole) in the aspect of the free energy for the formation of paired fragments. But this domination must be weakened by entropic factors, which are now difficult to estimate.

This structure could be stbilized by additional single tertiary pairs between loops b and d. For WG (Fig. 2c) the binding was C(57)-G(75) with an enthalpy of ca. 3 kcal/mole, whereas in the case of LS an additional binding between U(24) and G(75) with an enthalpy of ca. 1.5 kcal/mole is postulated.

Thermodynamic parameters

Enthalpy ΔH and entropy ΔS were analyzed separately for each pairing fragments predicted for the formation of RNA structures in order to interpret quantitatively the thermodynamic transitions observed by DSC. In this way, it was possible to determine the enthalpies ΔH of the melting of particular helical fragments, and to characterize their 'intrinsic' entropy (ΔS) resulting from the sequence in the helix and stacked nucleotides at the ends. However, this approach left out of consideration some additional entropic factors which result from a binding of the intertwined helical fragments with the unpaired fragments forming the loop.

Table 2 presents the results of calculations of the stability of helical fragments with the approach which assesses the potential stabilizing effect of nucleotides in the immediate neighborhood of the helix.

The thermal stability, i.e. the value of the temperature of untwisting of the structure (T_m) was calculated from a general dependence for free energy for each helix separately. The
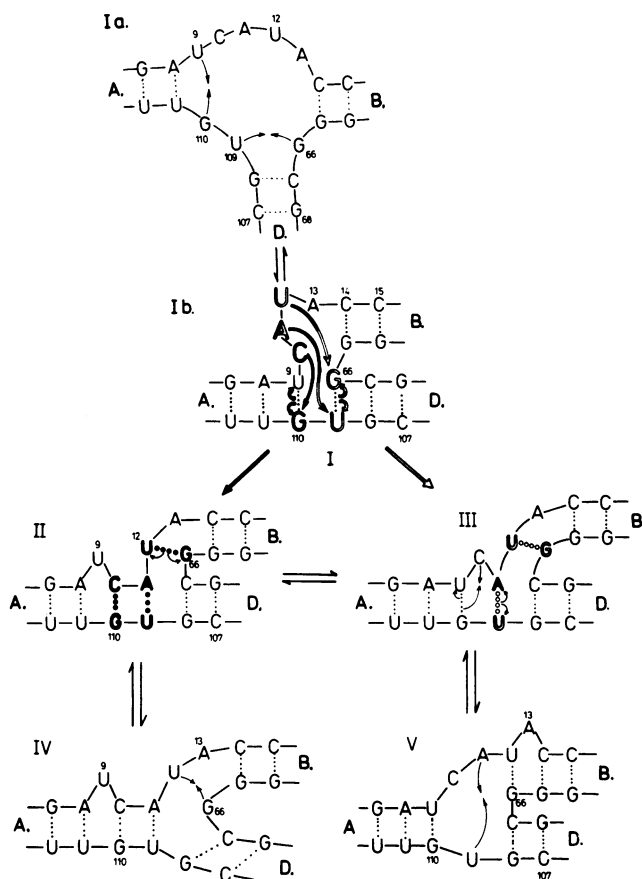
Fig. 3. The schematic presentation of the dynamism of forking loops 'a'. Description of transformation of I into other arrangements are in the text.

correction for experimental ionic conditions was performed according to Freier et al.[3].

Apart from different thermodynamic parameters which are due to an unlike secondary structure of helical fragments A, C', a difference is also found in fragment C, when the stacking of adjoining nucleotides is treated as a factor stabilizing the helix. In this aspect helical fragment C in WG possesses an enthalpy higher by 4.6 kcal/mole and greater thermal stability. Low temperature base paired fragments C_L and C'_L exist only in LS 5S rRNA.

DISCUSSION

The experimental values of enthalpy measured in the presence of a low concentration of Na^+ ions equalled 366 kcal/mole for 5S rRNA from WG and 398 kcal/mole from LS (see Table 1).

The values of the total enthalpy for the structure calculated theoretically from the nearest neighbour model including the stabilizing effect of the oligonucleotides directly adjacent to the ends of helices and entering into stacking interactions with them, are 355 kcal/mole for WG and 385 kcal/mole for LS (see Table 2). Those values already include the stabilizing contribution of the tertiary interaction between two fragments: (34−37) and (84−87) characterized by a value of 35 kcal/mole, and single tertiary bonds between loops 'b' and 'd'. Without those interactions they are lower by ca. 18 kcal/mole.

A congruency of the theoretically predicted enthalpy values with those measured experimentally justified the discussion of experimental data on the basis of an assumed theoretical model. Calculations of structure stability comprised possible tertiary interactions such as the pairing of single base pairs, which in a certain spatial configuration can form a stable bonding even at high temperature. The stabilizing effect of water mediated hydrogen bondings was omitted, though it can considerably contribute to the stability of tertiary structures [21].

An analysis of experimentally observed and potential components of structural transitions predicted theoretically from the model revealed that in spite of an externally diversified shape of the melting curves, they could be well described by the melting of very similar secondary and tertiary helical structures. Experimentally found differences are also clearly explained on the basis of thermodynamic differences derived from the primary structures of WG and LS 5S rRNA.

The correspondence of untwisting helical structures and particular structural changes for WG is presented in Table 3. Thermodynamically observed transitions are due to the unfolding of a single helical structure, or consist in a complex decomposition of two or more substructures. The assignment is made by combining both enthalpy values and temperatures of melting characterizing the model structures and thermodynamic parameters of the transitions observed.

5S rRNA from wheat germ

For 5S rRNA from WG helix B is theoretically the most stable one as far as temperature is concerned (52°) (see Table 3). The enthalpy of its melting equals 75 kcal/mole which is close to 87.6 kcal/mole determined for the thermally most stable transition in DSC analysis. The next constituent peak of the melting curve with an enthalpy of 112.8 kcal/mole corresponds to the sum of denaturation of two helical structures E and C, with enthalpies of 61 kcal/mole and 43 kcal/mole, respectively. The third peak with ΔH enthalpy of 96 kcal/mole corresponds to the untwisting of helices A and D with an enthalpy of 56.1 kcal/mole and 46.5 kcal/mole, respectively. The fourth peak at 35°C, with an enthalpy of 70 kcal/mole is attributed to the breaking of tertiary structure T1 with enthalpy equalling 34.9 kcal/mole as well as to the untwisting of structures C', D' and T2 with enthalpies of 28.4, 11.0 and 3 kcal/mole.

It is worth stressing that the temperatures of transitions T_m are congruent with the temperatures characteristic for the components of the experimental curve. The theoretical value of T_m (324 K) obtained for the most stable helical fragment B is equal to the experimental value (325 K).

DSC measurements for WG had already been performed by Marshall [10], who on the basis of structural calculations and an analysis of the shape of the DSC curve proposed another secondary structure for 5S rRNA. Our measurements of 5S rRNA from WG were performed under other ionic conditions, although those differences should not be critical for the molecular structure of 5S rRNA. The experiment of Marshall which most closely approximated the conditions used by us is the one conducted for a buffer containing 100 mM NaCl. The value of the total melting enthalpy of the structure equalled 371 kcal/mole for this sample. The decomposition of the DSC curve revealed the presence of 4 component transitions.

The total enthalpy value measured under our ionic conditions was 366 kcal/mole and is in agreement with the results of Marshall.

However, our interpretation of the experimental data is different. Our calculations of the enthalpy values for the predicted helical structures were performed on the latest results for the thermodynamic parameters of the RNA series, and varied from those used by Marshall. In principle, calculations of this type predict the minimal value of the bonding energy of the structure, which does not account for nontypical nonspecific tertiary interactions that are also potential contributors to the stability of a molecular structure and for this reason one may expect a discrepancy between theoretical and experimental data. The summaric value of the enthalpy predicted for secondary helical structures determined regardless of the postulated tertiary interactions would markedly differ from the experimental value, in spite of including the stabilizing effect of nucleotides adjacent to the ends of helices. However, when their impact to structure stability is taken into account, very good agreement between theoretical predictions and experiment is achieved.

5S rRNA from lupin seeds

Also for 5S rRNA from LS, the relationship between the observed components of the experimental melting profiles and the parameters of model 5S rRNA structure calculated in a semi−empirical way shows considerable congruency of the theoretically predicted properties and experimental data (Table 4).

The arrangement of the secondary structure and tertiary interactions in 5S rRNA from LS is almost identical to that of WG. Still, the thermodynamic image of particular structural fragments is different, and there are structural elements characteristic for particular sequences.

From thermodynamic parameters it follows that as far as temperature is concerned, helical domain A, with an enthalpy of 66.5 kcal/mole is the most stable fragment ($T_m = 58°C$) of this molecule. The experimentally observed structural transition with an enthalpy of 70.2 kcal/mole ($T_m = 56°C$) is attributed to the untwisting of this fragment. The change of stability of helical fragment A is crucial for the form of the melting curve and for a markedly greater stability of the whole molecule of 5S rRNA from LS. This is the essential thermodynamic difference between both types of 5S rRNA. The second constituent, (enthalpy $\Delta H = 147$ kcal/mole, $T_m = 50°C$), comprises a transformation of fragment B with an enthalpy of 75.0 kcal/mole like in 5S rRNA from WG and also the untwisting of helix E where the enthalpy is 61.1 kcal/mole.

The next, third component of the DS curve ($T_m = 47°C$), with enthalpy equalling 52.7 kcal/mole contains the destabilization of fragment D, with an enthalpy of 46.5 kcal/mole.

The subsequent difference is concealed in the fourth component, whose enthalpy equals 101 kcal/mole. It contains the untwisting of helix C, with an enthalpy of 38.6 kcal/mole and a tertiary T1 bonding with an enthalpy of 34.9 kcal/mole. The remaining contribution to constituent 4 consists in a breaking of fragments C' and D', their enthalpies being 21.0 and 11.0 kcal/mole, respectively.

Component transition 5 is attributed to the structural transition between two forms of helices C_L and C'_L at low temperature conformer 'a' into helices C' and C at high temperature conformer 'b' of LS−5S rRNA. The melting of helices C_L and C'$_L$ (see Fig.2a) leading to helices C and C' (see Fig. 2b), similar to analogous WG fragments (see Fig. 2c) could be accomplished by breaking six base pairs at 2a (21-UAAUGC-26 : 48-GCA(G)UUA-54) and forming three new base pairs

(25-GC-26 : 51-GU-52 and 29C : G48). These transitions are connected with an enthalpy change of 27 kcal/mole.

Analysis of the possible secondary structures of 5S rRNA shows also that the 'forking' loop 'a' linking helices A, B, and D (see Fig. 2) is an important element of the conformational dynamics of the whole molecule, probably influencing the three-dimensional orientation of helical segments (see Fig.3). An analysis of the sequence of this fragment revealed that there exist several alternative arrangements of the possible Watson-Crick and other types of interactions within this loop. They are of a general significance because the sequence of this fragment of 5S rRNA is conserved in all eukaryotic organisms. In Fig.3 we tried to demonstrate the potential dynamism of forking loops 'a' in four different arrangements: Ia, Ib, IV and V where one can see the real loops with unpaired bases: 8, 4, 3 and 3 respectively. As can be seen, we assume dynamic equilibrium beetwen arrangements Ia and Ib by the formation or breaking of hydrogen bonds between two mismatches GU at positions 9...110 and 66...109 which enlarge or diminish the 'a' loops from 4 (Ib) to 8 unpaired bases in Ia.

In our opinion arrangement Ib is quite ready to undergo a deeper transformation by formation of three or two new hydrogen bonded base pairs (G:C, A:U and U:G, or A:U and U:G) with a simultaneous breaking of two GU pairs. In such a case, Ib could be transformed into arrangement II or III which in reality loses the loop character extending the B helix by one and A helix by one or two additional base pairs with two new single bulges (at U9 and A13 in II and C10 and A13 in III structures).

Arrangement II could be in dynamic equilibrium with arrangements IV and III and the latter with arrangement V. All these hypothetical transformations are shown schematically in Fig. 3.

Arrangement II, having the possibilities of easy and direct transformations into III and IV could be more favourable than both standard structures Ia and Ib.

A direct closing of helices A and D by terminal mismatches GU (see Fig. 3 Ib) does not introduce any bulges, but creates an asymmetrical loop of 4 unpaired nucleotides. Under these conditions the stacking interaction between helices A and D seems to be less stable. This loop may also possess a dynamic conformation with the interaction of G66 flipping between U12 and U109 which may provide the driving force for a structural transformation of the whole molecule during the functional interactions of 5S rRNA.

The presented calculations of the stability show the thermodynamic preference for structure Ib. They are based on the empirical thermodynamic data for secondary structure formation, not including any three dimensional stabilizing factors. In that respect they correspond very well to the presented experimental results, where only monovalent ions are the stabilizing effectors.

These equilibrium of the structure may be influenced by any steric interaction within the loop 'a', for example by specific protein interaction and/or other counter ions binding, but then a real, local three dimensional structure has to be considered in discussed interactions.

FINAL REMARKS

The thermal stability of the molecular structures of two plant 5S rRNAs: from wheat germ and lupin seeds have been compared. Differences in the sequence structure do not lead to important

differences in their predicted (model) secondary and tertiary structure. Both types of 5S rRNA can form secondary structures on the basis of 5 helical fragments, and tertiary interactions in identical positions, although some differences in the structural dynamics appear as an effect of differences in the sequences.

The sequence differences are cumulated in helical fragment A (6 out of 8 differences), and one is found in the immediate vicinity of helix C (position 24) and the last (position 49),— within that helix. The difference in position 24 and 49 influences the structure of fragments C' and C (compare Fig. 2a with 2c).

The differences observed in DSC melting profiles for 5S rRNA of both types can be explained by reference to the model molecular structure. Differences in the sequence of fragment A cause drastic changes in the thermal stability of this molecular fragment. For both the 5S rRNA considered, temperature T_m, characterizing the untwisting of this structural fragment is shifted by ca. 14°. At enthalpy values of 56.1 kcal/mole for WG and 66.5 kcal/mole for LS (which amount to almost 20% of the total enthalpy of transition for 5S rRNA) such a large shift of T_m results in drastically various forms of DSC curves—from a one peak curve (WG) to a curve with 2 clearly formed peaks (LS) (Figs. 1a and 1b).

A comparative analysis of DSC curves and the theoretical predictions based on the model of secondary structure and tertiary H-bonding pattern made it possible to establish a reliable relationship between the profiles of the melting curves and the structure and the predicted stability of its particular helical fragments.

The proposed secondary structure is in accordance with the general structure of 5S rRNA models for the Eukaryotes [2], and resembles the schemes proposed by Fox and Woese [22] and Studnicka et al. [23].

We propose another organization of the nucleotides found between helix B and loop c. This fragment, in which differences in the sequences appear in eukaryotic organisms, may form a flexible element of the structure, differentiated for various organisms. Formation of different helices C and C' seem to be clearly confirmed by our results.

The enlargement of thermodynamically favored hairpin loop 'e' opens the way for a possible tertiary interaction with hairpin loop c, by 4 pairs: CG CG CG AU, as proposed by Joachimiak et al. [24].

Our consideration of the structure with a simple flexible mechanical model shows that both pairing are sterically permissible for the model 5S RNA structure in this region— antiparallel (C34-A37)—(G87-U84) or parallel (C34-A37)— (G85-U88), but the antiparallel one seems to be more adequate in the sense of the fitness of the entire modelled structure.

This interaction may be strengthened by an additional single pairing of loops 'b' and 'd'. A better tertiary stability and greater stability of fragment A for LS 5S rRNA probably lead to an increase of nonspecific tertiary interactions, which in an apparent way further stabilize its structure in low temperatures.

The assumed structural model is well consistent with the experimental data described above. The enthalpy of this structure, taking into account the postulated tertiary interactions, has been calculated on the basis of effects connected with base pairing and gave results congruent with those observed by experiment. But this does not definitely exclude the structural model, in which the extension of helical region E could dominate over the postulated tertiary interaction between hairpin loops due to interactions stronger than those predicted by standard thermodynamic parameters, induced for example by a specific ion binding. The summaric energetic data for both situations are quite similar and only a precise analysis supported by another experimental technique may definitively solve which structure is real, and under what conditions it is formed.

REFERENCES

1. Erdman, V.A. (1976) Prog. Nucl. Acids Res. Mol. Biol. **18**, 45—90.
2. Erdman, V.A., Wolters, J. (1986) Nucleic Acids Res. **14**, r1—59.
3. Freier, S.M., Petersheim, M., Hickey, D.R., Turner, D.H. (1984) J. Mol. Struct. Dyn. **1**, 1229—1242.
4. SantaLucia, J., Kierzek, R., Turner, D. (1990) Biochemistry **29**, 37—44
5. Barciszewska, M., Lorenz, S., Erdmann, V.A., Barciszewski, J. (1990) Biochim. Biophys. Acta ,**1087**, 68—72.
6. Aubert, M., Scott,J.F., Reynier, M., Monier, M. (1968) PNAS USA **61**, 292—299.
7. Woese, C.R., Pribula, C.D., Fox, G.E., Zablen, L.B. (1975) J. Mol. Evolution **5**, 35—46.
8. Kime, M.J., Moore, P.B. (1982) Nucleic Acids Res. **10**, 4973—4983.
9. Matveev, S.V., Filimonov, V.V., Privalov, P.L. (1982) Mol. Biol. **16**, 990—999.
10. Shi Jiang Li, Marshall, A.G. (1985) Biochemistry **24**, 4047—4052.
11. Lee-Hong Chang, Marshall, A.G. (1986) Biopolymers **25**, 1299—1313.
12. Barciszewski, J., Bratek-Wiewiórowska, M.D., Górnicki, P., Naskret-Barciszewska, M., Wiewiórowski, M., Zielenkiewicz, A. and Zielenkiewicz, W. (1988) Nucleic Acids Res. **16**, 685.
13. Barciszewska, M.Z., Mashkova, T.D., Zwierzynski, T., Kisselev, L.L. and Barciszewski, J. (1986) Bull. Pol. Acad. Sci., Chem. **34**, 369—373.
14. Rafalski, J., Wiewiórowski, M. and Soll, D. (1982) Nucleic Acids Res. **10**, 7635—7642.
15. Privalov, P.L., Plotnikow, V.V., Filimonov, V.V. (1975) J. Chem. Termodyn. **7**,41—47.
16. Freire, E., Biltonen , R.L. (1978) Biopolymers **17**, 463.
17. Chang, L.H., Li, S.J., Ricca, T.L., Marshall, A.G. (1984) Anal. Chem. **56**, 1502—1507.
18. Zuker, M., Stigler, P. (1981) Nucleic Acid Res. **9**, 133—148.
19. Kim, K., Jhon, M. S. (1979) Biochim. Biophys. Acta **565**, 131—147.
20. Turner, D.H., Sugimoto, N., Freier, S.M. (1988) Ann. Rev. Biophys. Chem. **17**, 167—192.
21. Westhof, E. (1988) Ann. Rev. Biophys. Chem. **17**, 125—144.
22. Fox, G.E., Woese, C.R. (1975) J. Mol. Evolution **6**, 61—76.
23. Studnicka, G.M., Eiserling, F.A., Lake, J.A. (1981) Nucleic Acids Res. **9**, 1885—1904.
24. Joachimiak, A., Nalaskowska, M., Barciszewska, M., Mashkova, T., Barciszewska, J. (1990) Int. J. Biol. Macromol. **12**, 321—327.